Light-Driven Chloride Ion Transport by Halorhodopsin from *Natronobacterium pharaonis*. 2. Chloride Release and Uptake, Protein Conformation Change, and Thermodynamics[†]

György Váró,[‡,||] Richard Needleman,[§] and Janos K. Lanyi[‡,*]

Department of Physiology and Biophysics, University of California, Irvine, California 92717, and Department of Biochemistry, Wayne State University School of Medicine, Detroit, Michigan 48201

Received June 28, 1995; Revised Manuscript Received September 5, 1995[⊗]

ABSTRACT: The photocycle of the light-driven chloride pump, *N. pharaonis* halorhodopsin, is described by the scheme $HR \xrightarrow{h\nu} K \rightarrow \leftrightarrows L \leftrightarrows N \leftrightarrows O \leftrightarrows HR' \rightarrow HR$. From the chloride dependencies of the rate constants in this model we identify the N → O and O → HR′ reactions as the steps where chloride release and uptake occur, respectively, during the transport. The dependencies of the rate constants on temperature describe a thermodynamic cycle in which enthalpy−entropy conversion occurs in the O → HR′ reaction. The dependencies of the rate constants on hydrostatic pressure indicate that a substantial volume *decrease* occurs at the L → N reaction, a result of a large-scale conformational change. This is the opposite of the volume *increase* in the photocycle of the proton pump, bacteriorhodopsin, that is implicated in the access change of the active site during the transport and the passage of a proton from the cytoplasmic surface to the active site. The results together suggest a chloride transport mechanism, in which the equivalents of all the ion transfer steps in bacteriorhodopsin occur but in the reverse sense, so as to cause the extracellular-to-cytoplasmic translocation of a chloride ion instead of the cytoplasmic-to-extracellular transport of a proton.

In the preceding paper (Váró et al., 1995b) we described the photochemical reaction cycle of halorhodopsin from *Natronobacterium pharaonis*. This light-activated chloride ion pump (Bivin & Stoeckenius, 1986; Duschl et al. 1990; Lanyi et al. 1990; Scharf & Engelhard, 1994) is analogous to the earlier studied halorhodopsin from *Halobacterium salinarium* (reviewed by Lanyi, 1986, 1990; Oesterhelt & Tittor, 1989; Oesterhelt et al., 1992), and the increasing number of other halorhodopsins found in other halophilic archae (Otomo et al., 1992; Soppa et al., 1993). Our intention in comparing these chloride pumps with bacteriorhodopsin, the light-activated proton pump in this group of organisms, is to dissect the properties relevant to the mechanism of active ion translocation from those that determine ion specificity. The recent finding that the D85T single-residue replacement converts bacteriorhodopsin to a chloride ion pump (Sasaki et al., 1995) encourages us to believe that separation of these two aspects of the transport will be possible.

Its somewhat different properties promise to make *N. pharaonis* halorhodopsin, rather than the *H. salinarium* protein, the system of choice for studying the chloride transport mechanism. The advantages of this system (Váró et al., 1995b) are that (1) the chromophore does not undergo light/dark adaptation that would complicate the study of the transport-active all-*trans* retinal−containing form (Váró et al., 1995a), and the spectral changes after photoexcitation contain little or no contribution from the 13-*cis* chromophore; (2) spectroscopic titration of the chromophore with chloride suggests a simple two-state equilibrium and describes a binding site near the Schiff base with a K_D of 1 mM; (3) the photocycle kinetics change with chloride concentration well above 1 mM (between 0.1 M and 2 M, as described in Váró et al., 1995b), in a way that should reveal the details of chloride uptake and release during the transport; and (4) at 0.1 M chloride the photocycle resembles that of the D85T mutant of bacteriorhodopsin (Sasaki et al., 1995) that had acquired the chloride transport function.

In this paper we report our studies in which these properties of *N. pharaonis* halorhodopsin are exploited to obtain a first, tentative kinetic and mechanistic scheme for the chloride transport. The photocycle steps associated with chloride release and uptake were inferred from the dependence of two of the rate constants on chloride concentration. Protein conformational changes were placed into the photocycle scheme by identifying the steps affected by hydrostatic pressure up to 1 kbar, and their nature was suggested from the directions of these effects. The thermodynamic cycle was described from the temperature dependencies of the rate constants, as earlier for bacteriorhodopsin (Váró & Lanyi, 1991a,b). From the results, we propose that the mechanism of chloride transport is similar in principle to proton transport in bacteriorhodopsin, and the main difference from the other pump is that the elementary events that translocate the chloride occur in the reverse direction.

[†] This work was funded by grants from the National Institutes of Health (GM 29498 to J.K.L.), the Department of Energy (DEFG03-86ER13525 to J.K.L. and DEFG02-92ER20089 to R.N.), and the National Science Foundation (MCB-9202209 to R.N.).

* To whom all correspondence should be addressed.

[‡] University of California.

[§] Wayne State University School of Medicine.

[||] Permanent address: Institute of Biophysics, Biological Research Center of the Hungarian Academy of Sciences, H-6701 Szeged, Hungary.

[⊗] Abstract published in *Advance ACS Abstracts,* October 15, 1995.

0006-2960/95/0434-14500$09.00/0

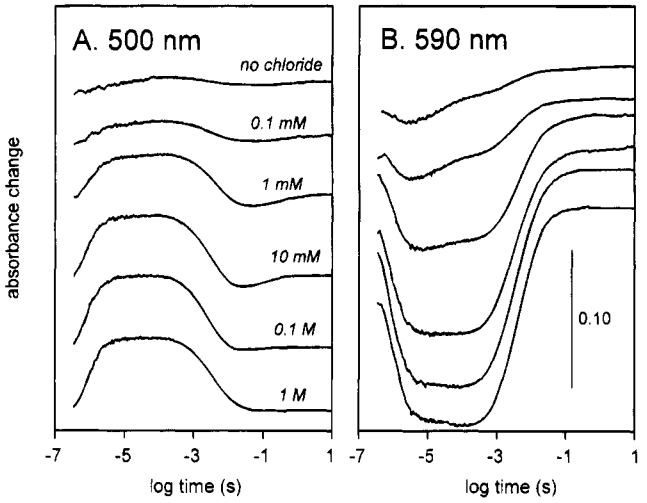

FIGURE 1: Absorbance changes *vs.* time after photoexcitation of *N. pharaonis* halorhodopsin at various chloride concentrations: (A) 500 nm; (B) 590 nm. The chloride concentrations, adjusted by mixing 2 M NaCl with 1 M Na_2SO_4, so as to keep the Na^+ concentration at constant 2 M, are given in A.

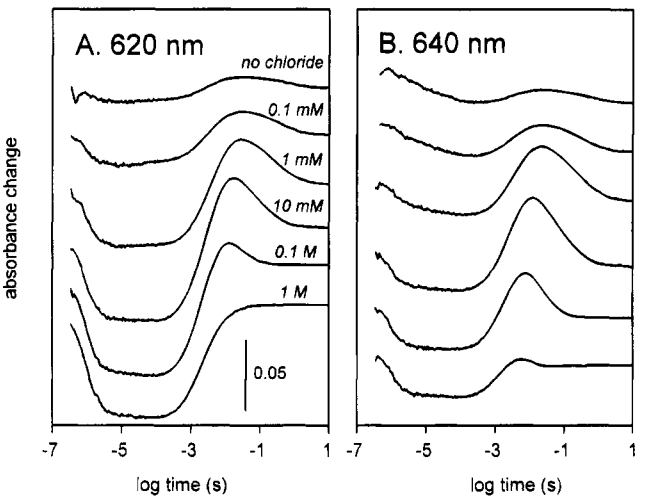

FIGURE 2: Absorbance changes *vs.* time after photoexcitation of *N. pharaonis* halorhodopsin at various chloride concentrations: (A) 620 nm; (B) 640 nm. The chloride concentrations, adjusted by mixing 2 M NaCl with 1 M Na_2SO_4, so as to keep the Na^+ concentration at constant 2 M, are given in A.

MATERIALS AND METHODS

Preparation of cell membranes containing cloned *N. pharaonis* halorhodopsin, and the sample conditions were described in the preceding paper (Váró et al., 1995b). Absorbance changes after flash photoexcitation were measured at single wavelengths as before (Váró et al., 1995a), except that a photomultiplier with extended sensitivity in the red was used. The buffer was 50 mM MES,[1] pH 6.0, throughout, in addition to the other salts present as specified. The temperature was controlled at 22 °C, except in studies of the temperature and pressure dependencies. Since these samples do not show light/dark adaptation (Váró et al., 1995b), no precautions needed to be taken to light-adapt them. Global fitting of kinetic schemes to the time course of absorbance changes at several (four) single wavelengths was with the program RATE, written by G. Groma. This software utilizes the extinctions for halorhodopsin and its photointermediates, derived from data measured with an optical multichannel analyzer as described earlier (Zimányi et al., 1989; Zimányi & Lanyi, 1993), and yields the rate constants of the best fits.

Pressure dependence of the photocycle was studied by performing the spectroscopic measurements in a pressure cell from ISS (Champaign, Illinois) with three windows, two for the entry and exit of the measuring light and the third for the actinic laser flash.

RESULTS

Chloride Dependencies of the Photocycle Reactions. The photocycle was examined at various chloride concentrations, adjusted by mixing 2 M NaCl and 1 M Na_2SO_4, keeping thereby the concentration of Na^+ constant. Figures 1 and 2 show the time courses of absorbance changes after photoexcitation, followed at 500, 590, 620, and 640 nm. It is evident from Figure 1 that at wavelengths below 600 nm, particularly at 500 nm, the kinetics are unaffected by chloride, except for the amplitudes of the changes (increase at 500 nm and decrease at 590 nm) consistently with the chloride-binding equilibrium of the unphotolyzed state (Váró et al., 1995b) between zero and 10 mM chloride. The kinetics at 620 and 640 nm reflect this equilibrium as well (Figure 2), but in addition the large absorbance increase in the millisecond time range loses amplitude considerably at the higher chloride concentrations and its decay is accelerated.

Since the binding of chloride that determines the absorption maximum of the chromophore (Váró et al. 1995b), and the occurrence of the "chloride-type" photocycle upon photoexcitation (cf. below) are both described with a K_D of 1 mM, no photoproducts from the nonbinding form will be present at chloride concentrations above a few tens of mM. The chloride dependencies of individual reactions in the "chloride-type" photocycle were therefore examined at chloride concentrations greater than 30 mM. The scheme K ⇔ L ⇔ N ⇔ O ⇔ HR′ → HR (Váró et al., 1995b) was fitted to single wavelength traces, such as in Figure 1 and 2, but measured at numerous chloride concentrations up to 2 M. Figure 3 shows the rate constants of the best fit as functions of the chloride concentration. Figures 4A and B illustrate the quality of the fits for data at 0.1 M and 2 M chloride, respectively (for the sake of clarity the 590-nm traces are omitted). We arrived at the model in the following way. The fits to the last decay process at 620 and 640 nm at chloride concentrations below 1 M required a scheme with two exponential processes. We tried a number of models that allowed for such kinetics. As mentioned in the preceding paper (Váró et al., 1995b), fitting a scheme in which the decay of N to HR is via two pathways, one directly and the other through O, was not satisfactory. The scheme containing K ⇔ L ⇔ N and two O states, each produced from N and each decaying to HR, fit the data well, as did the K ⇔ L ⇔ O ⇔ N → HR and the K ⇔ L ⇔ N ⇔ O ⇔ HR′ → HR sequences. In the last scheme, the decay of O is through an equilibration reaction with an HR-like state, analogous to the decay of the M state in bacteriorhodopsin, where the first component of the decay is interpreted (Otto et al., 1989; Zimányi et al., 1993) as the equilibration of M with N, and the second as the decay of the M *plus* N mixture.

[1] Abbreviations: K, L, N, and O are intermediates of the photocycle of halorhodopsin, and are analogous to the intermediates of bacteriorhodopsin which include also M; MES, 2-[2-morpholino]ethanesulfonic acid.

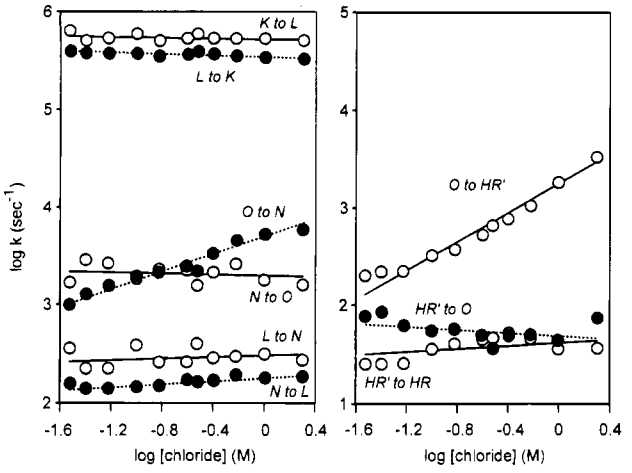

FIGURE 3: Rate constants vs. chloride concentration for the K ⇌ L ⇌ N ⇌ O ⇌ HR′ → HR scheme, fitted globally to data similar to those in Figures 1 and 2. The rate constants of the forward reactions, as written, are shown with open circles and solid lines, those of the back-reactions with closed circles and dotted lines.

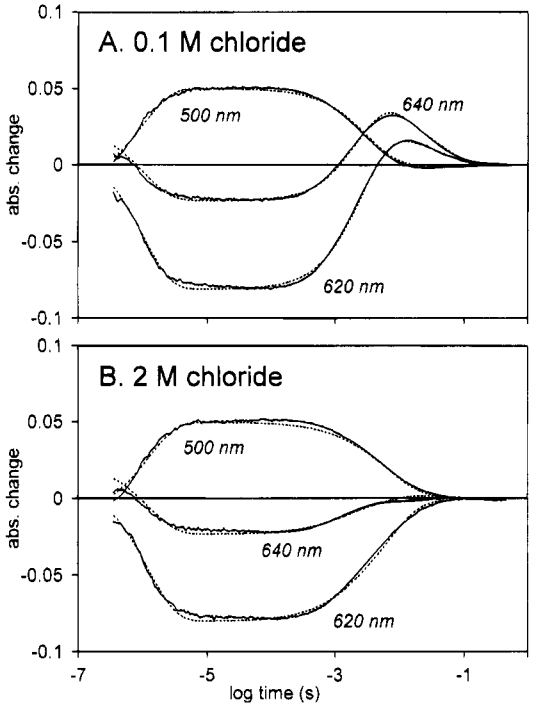

FIGURE 4: Fits of the K ⇌ L ⇌ N ⇌ O ⇌ HR′ → HR scheme to the measured time-dependent absorbance changes under two conditions. (A) 0.1 M NaCl + 0.95 M Na_2SO_4; (B) 2 M NaCl. Solid lines, data, dotted lines, best fits of the model.

Deciding among these models was on the basis of the mechanistic consideration that we expect one uptake step (which should be dependent linearly on chloride concentration) and one release step (whose reverse ought to be chloride dependent) in a transport cycle. With this criterion all but the last model were eliminated because too many steps were dependent on chloride, and not sufficiently to ascribe their dependence as originating from chloride uptake (not shown).

It is evident from Figure 3 that in the remaining scheme only two of the rate constants are significantly dependent on chloride concentration. The simplest interpretation of these chloride dependencies is that they reflect the first-order kinetics for chloride expected for chloride uptake. The logarithms of the rate constants of the O → HR′ forward reaction and the O → N back-reaction *vs.* the logarithms of the chloride concentration have slopes of 0.75 and 0.47, respectively. A slope of 0.75 describes also the amplitude of spectral shift of the unphotolyzed chromophore upon binding of chloride (Váró et al., 1995b). The origin of what appears to be a reaction order of 0.75 for the chloride binding and the chloride uptake is not clear, but it may not be a coincidence that the pH dependencies of processes that reflect proton binding to the extracellular surface of bacteriorhodopsin also have slopes of 0.7−0.8 (Marti et al., 1992; Cao et al., 1995). The lesser slope of 0.47 for the reverse of the chloride release step in the model is likewise unexplained, but suggestively, the pH dependence of proton uptake on the cytoplasmic surface in the photocycle of D96N bacteriorhodopsin has a similar slope, between 0.3 and 0.5 (Tittor et al., 1989; Miller & Oesterhelt, 1990; Cao et al., 1991). If these deviations from first-order ion binding have a common origin, it must be that protons and chloride both bind cooperatively with respect to the fixed charges at the membrane surface and affect the surface potential (Alexiev et al., 1994; Cao et al., 1995).

The intercept of the line for the rate constant of the O → HR′ reaction and that for the reverse HR′ → O reaction (Figure 3) gives an apparent binding constant of 10−15 mM for chloride in this postulated equilibrium. The O → HR′ reaction would be therefore the step where chloride is taken up in the photocycle, with a K_D of 10−15 mM. Likewise, the chloride dependence for the O → N back-reaction implies that its reverse, the N → O reaction, is where chloride is released in the photocycle. The apparent binding constant for chloride in this equilibrium is about 0.15 M. Although these experiments do not reveal which side these binding equilibria take place, we assume from the direction of the transport (Schobert & Lanyi, 1982) that the uptake is at the extracellular surface and the release is from the cytoplasmic side.

The rate constants of the early steps in the photocycle are unaffected by chloride, and the absorbance changes in the tens of microseconds time-range are influenced by chloride only in their amplitudes. This occurs at chloride concentrations that reflect the binding of chloride to the site that elicits the "chloride-type" photocycle. Figure 5 shows the amplitudes at 500, 590, 620, and 640 nm (normalized to 1 between zero and 2 M chloride) *vs.* the logarithm of chloride concentration. Also shown are the normalized amplitudes of the spectral shift of the unphotolyzed chromophore (Váró et al., 1995b). The binding constant that describes all of these parameters is 1 mM, and the apparent order of the binding reaction is 0.75 (dotted line).

Thermodynamic Parameters of the Photocycle. For bacteriorhodopsin the enthalpies and entropies of activation of the photocycle reactions, as well as the free energies of activation at a given temperature, had been calculated from the temperature dependencies of the rate constants (Váró & Lanyi, 1991a,b). We have done such an analysis for halorhodopsin as well. Figure 6 shows absorbance changes at 500, 590, and 640 nm after photoexcitation at 10, 15, 20, 25, and 30 °C. The K ⇌ L ⇌ N ⇌ O ⇌ HR′ → HR scheme was fitted globally to these traces, as well as another set measured at 620 nm (not shown), and the rate constants of the best fit are shown as Eyring plots in Figure 7. The temperature dependencies are described satisfactorily by straight lines. The slopes yield $\Delta H^{\ddagger}$, and the intercepts $\Delta S^{\ddagger}$ for each reaction. Since all reactions, except the initial one

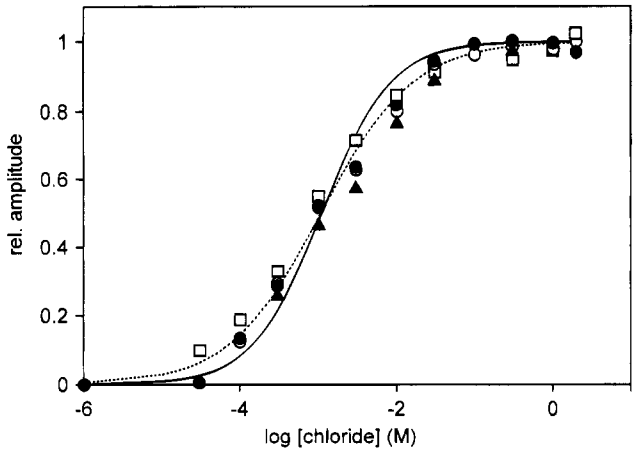

FIGURE 5: Chloride dependencies of various parameters of *N. pharaonis* halorhodopsin. Symbols: (○), absorbance change at 500 nm; (●), 590 nm; and (▲) 640 nm, at their maximal amplitudes near 10 μs, scaled to give 0 and 1 at zero and 2 M NaCl, respectively; (□), amplitudes of the chloride-dependent spectral change of the unphotolyzed chromophore from Figure 1B in (Váró et al., 1995b). Solid line: best fit of a titration curve with first-order binding of chloride; dotted line: best fit with 0.75-order binding.

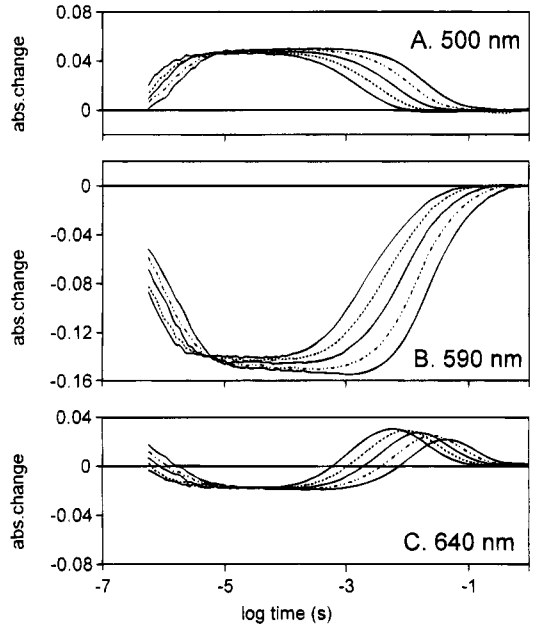

FIGURE 6: Temperature dependencies of absorption changes after pulse photoexcitation, measured at 500 nm (A), 590 nm (B), and 640 nm (C). Temperatures: —, 10 °C; —··—··—, 15 °C; —, 20 °C; ···, 25 °C; —, 30 °C.

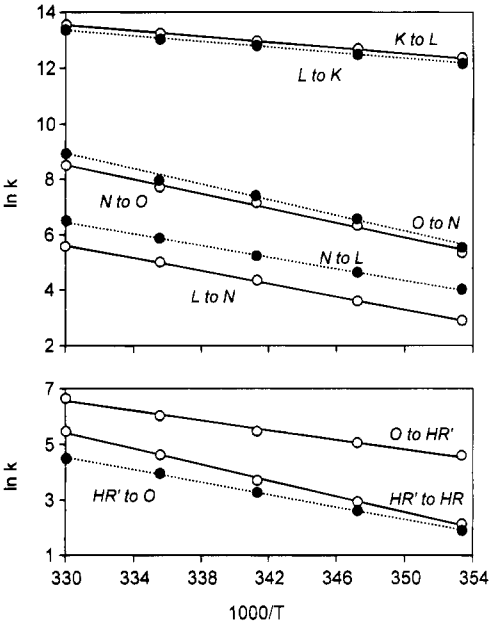

FIGURE 7: Eyring plot of the rate constants between 10 and 30 °C. The rate constants of the forward reactions are shown with open circles and solid lines, those of the back-reactions with closed circles and dotted lines. They were calculated from the data in Figure 6 and an additional set at 620 nm.

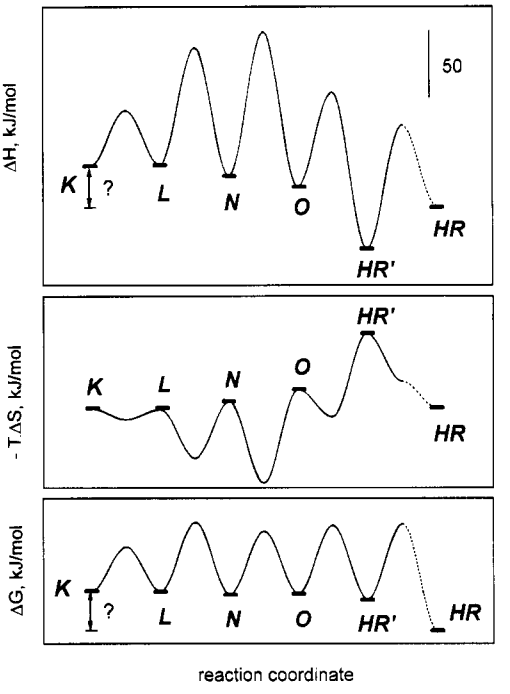

FIGURE 8: Enthalpy, entropy, and free energy changes in the photocycle of *N. pharaonis* halorhodopsin. The thermodynamic parameters of the measured reactions were calculated from the plots in Figure 7. The enthalpy (and therefore free energy) difference between the K and HR states is not known, and given arbitrarily. The dotted lines signify the fact that the activation parameters of the HR to HR′ back-reaction are not measurable. However, as for bacteriorhodopsin (Váró & Lanyi, 1991a), we assumed that little if any entropy change has occurred in the short time (nanoseconds) of the rise of the K state.

that produces K and the final one that recovers the unphotolyzed state, are reversible in the scheme, these parameters define the relative enthalpy, entropy, and free energy levels of the photointermediates as well. However, the thermodynamic parameters of K relative to HR are not known.

Figure 8 shows the calculated ΔH, $-T\cdot\Delta S$, and ΔG at 0.1 M chloride and 20 °C. There are several features to note. First, the activation enthalpies of all reactions exceed the activation free energies. Thus, none of the transition state have lower entropy, *i.e.*, are more highly organized, than the stable states that precede them. Thus, all barriers are enthalpic in nature. This is not so in the bacteriorhodopsin photocycle (Váró & Lanyi, 1991a,b). Second, there is a large enthalpy decrease, compensated by an entropy decrease (increase in $-T\cdot\Delta S$) so as to conserve free energy, in the O → HR′ reaction. Such an enthalpy−entropy conversion was a noted part of the thermodynamic cycle of bacteriorhodopsin (Váró & Lanyi, 1991a). Third, all reactions except the initial one that produces K and the final one that recovers the

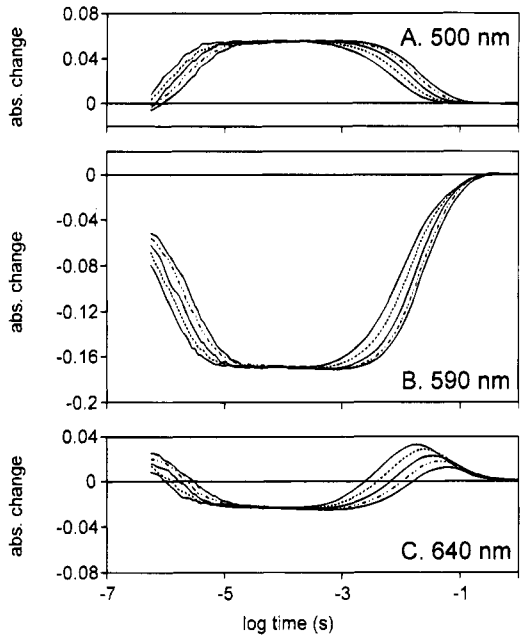

FIGURE 9: Pressure dependencies of absorption changes after pulse photoexcitation, measured at 500 nm (A), 590 nm (B), and 640 nm (C). Hydrostatic pressures: —, 1 bar; —•••—, 250 bar; —, 500 bar; •••, 750 bar; —, 1000 bar. Conditions: 100 mM NaCl, 0.95 M Na_2SO_4, 50 mM MES, pH 6.0, 20 °C.

unphotolyzed state, proceed with little change in free energy. This a property of an efficient catalytic cycle (Albery & Knowles, 1976).

Volume Changes in the Photocycle Reactions. Protein conformational changes will affect volume through changes in the internal packing geometry of residues and/or the binding of water (Heremans, 1982; Gross & Jaenicke, 1994). The rate constants in the bacteriorhodopsin photocycle are affected by hydrostatic pressure (Váró & Lanyi, 1995), as well as osmotic pressure (Cao et al., 1991). Although the interpretation of the pressure effects may be complicated by their possible influence also on the internal viscosity of the purple membranes (Marque & Eisenstein, 1984), our recent detailed analysis of the dependence of rate constants on hydrostatic pressure (Váró & Lanyi, 1995), correlated the largest effect with the conformation change in the cytoplasmic half of bacteriorhodopsin measured earlier by diffraction (Subramaniam et al., 1993). Thus, an about 32 cm^3/mole volume increase at the $M_1 \rightarrow M_2$ reaction was associated with what appear to be changes in dispositions of helices in the cytoplasmic half of the protein, including perhaps a tilt of helix F away from the intrahelical cavity that contains the retinal. Additionally, there was a large positive activation volume in the $M_2 \leftrightarrows N$ equilibrium, that implied a requirement of increased hydration for stabilizing the transition state in the proton transfer between D96 and the Schiff base, as suggested earlier also from the influence of osmotic agents (Cao et al., 1991). We have explored the effects of hydrostatic pressure also in the halorhodopsin photocycle.

Figure 9 shows absorbance changes measured at 500, 590, and 640 nm after photoexcitation at 1, 250, 500, 750, and 1000 bar. The $K \leftrightarrows L \leftrightarrows N \leftrightarrows O \leftrightarrows HR' \rightarrow HR$ scheme was fitted globally to these traces, as well as another set measured at 620 nm (not shown), and the rate constants of the best fit are shown as functions of pressure in Figure 10. The pressure dependencies are described by straight lines,

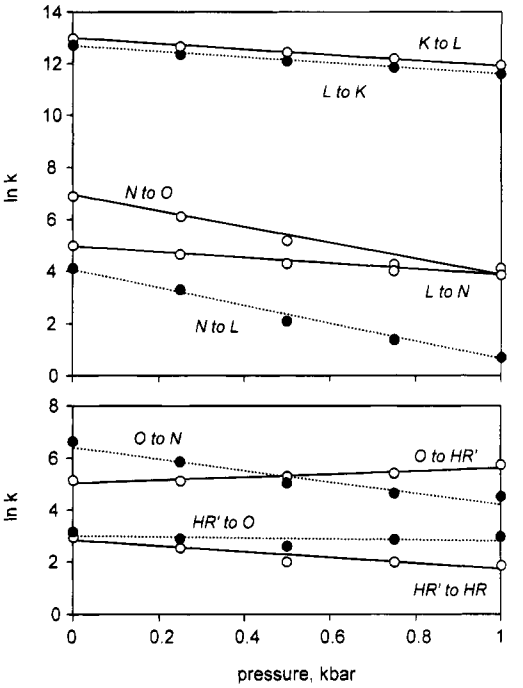

FIGURE 10: Pressure dependencies of the rate constants between 1 and 1000 bar. The rate constants of the forward reactions are shown with open circles and solid lines, those of the back-reactions with closed circles and dotted lines. They were calculated from the data in Figure 9, and an additional set at 620 nm.

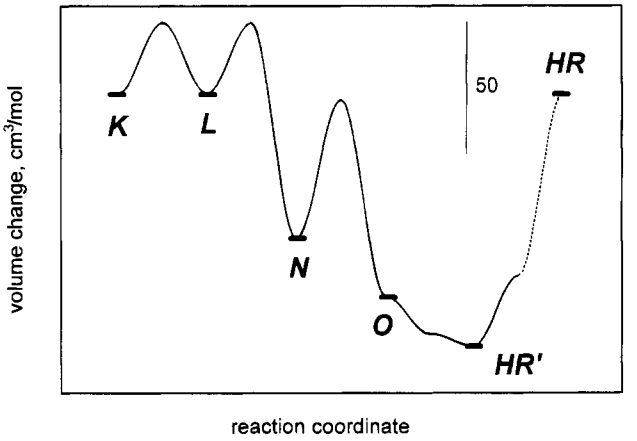

FIGURE 11: Volume changes in the photocycle of *N. pharaonis* halorhodopsin, calculated from the pressure dependencies of the rate constants (Figure 10). The dotted line signifies the fact that the activation volume of the HR to HR′ back-reaction is not measurable. We have assumed that the volume of K is not significantly different from the unphotolyzed HR state.

as expected (Heremans, 1982; Gross & Jaenicke, 1994). The slopes yield the negative of the volume change in the transition state, $\Delta V^{\ddagger}$, for each reaction. The calculated volume changes are shown graphically in Figure 11. For most reactions $\Delta V^{\ddagger}$ is near zero or positive, but the $O \rightarrow HR'$ reaction has a negative activation volume. The results indicate furthermore that the volumes of the N, O, and HR′ states, but not K and L, are 60−80 cm^3/mol smaller than the unphotolyzed state. Instead of a volume *increase* in the photocycle, as in bacteriorhodopsin, there is a volume *decrease*. If the volume change originates from a protein conformational change analogous to that in bacteriorhodopsin, the structural shift occurs in the $L \rightarrow N$ reaction and results in a more closed conformation relative to the unphotolyzed state rather than a more open one. We show

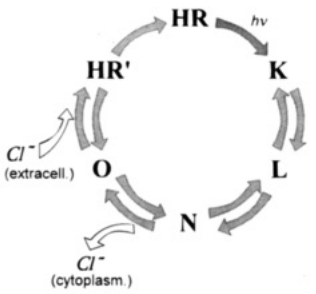

FIGURE 12: Photocycle scheme for halorhodopsin from *N. pharaonis*. FTIR spectra of N and O (Váró et al., 1995b) indicated that, as in K and L (Fodor et al., 1987; Rothschild et al., 1988), the retinal is 13-*cis* in N, but as in the unphotolyzed state, the retinal in O is all-*trans*. The chloride release and uptake steps are inferred from the dependencies of the O → N and O → HR′ reactions on chloride concentration (Figure 3). The suggested directions of the release and uptake would explain the net translocation of chloride from the extracellular to the cytoplasmic side during the transport cycle.

the reversal of this volume decrease in the HR′ → HR reaction in Figure 11 because the activation volumes of the earlier steps do not reveal its location, and it is the only unidirectional reaction where it could occur. However, we note that since the O → HR′ reaction is limited by chloride concentration (Figure 3), the activation volume we measure might not refer to a protein change that could take place, but to the requirements for the uptake of the chloride. It is possible therefore, that the initial volume recovers already in the HR′ state, and not as shown in Figure 11. As for the activation volumes, as in the bacteriorhodopsin photocycle (Váró & Lanyi, 1995), there is one step, here the N ⇔ O equilibrium, that has a rather large positive $\Delta V^{\ddagger}$.

DISCUSSION

The results we report here define a reasonable kinetic scheme for the photocycle of *N. pharaonis* halorhodopsin, and how the internal chloride translocation steps, as well as the release and uptake of chloride at the two membrane surfaces, are coupled to the chromophore reactions. The photocycle scheme we suggest is HR $\xrightarrow{h\nu}$ K ⇔ L ⇔ N ⇔ O ⇔ HR′ → HR. According to the chloride dependencies of the rate constants (Figure 3), the N → O reaction is associated with chloride release and the O → HR′ reaction with chloride uptake. This photocycle is illustrated in Figure 12. Together with the thermodynamics (Figure 8), and the volume changes inferred from the dependence of the rate constants on hydrostatic pressure (Figure 11), this scheme suggests a plausible chloride translocation mechanism, as described in the following.

In evaluating the results for halorhodopsin we were influenced by our current view of how bacteriorhodopsin transports protons. In this protein the first proton transfer after photoisomerization of the retinal is from the Schiff base to the anionic D85. This has two consequences. First, a proton in the extracellular domain is mobilized and becomes released to the surface (Liu, 1990; Liu et al., 1990; Heberle & Dencher, 1992; Zimányi et al., 1992). Second, the loss of coulombic interaction between the Schiff base and its counter-ion initiates a conformational rearrangement (Kataoka et al. 1994) that breaks the connection of the Schiff base to the extracellular side and establishes a new connection with the cytoplasmic side and the protonated D96 (the "reprotonation switch"). The conformational shift is more specifically described by diffraction changes (Dencher et al., 1989; Koch et al., 1991; Nakasako et al., 1991; Subramaniam et al., 1993; Han et al., 1994; Kataoka et al., 1994) that suggest movement and/or reorganization of the helical structure in the cytoplasmic half of the protein that exposes the interhelical cavity to a greater degree to the aqueous medium. These structural changes are likely to be responsible for the sensitivity of the reactions in the second half of the photocycle to temperature [indicating large changes in enthalpy and entropy levels (Váró & Lanyi, 1991b)], hydrostatic pressure [indicating a transient volume increase (Váro & Lanyi, 1995)], and water activity [indicating transient entry of water into the structure (Cao et al., 1991)]. Protein changes detected by changes in the amide band frequencies and amplitudes (Rothschild et al., 1981; Braiman et al., 1991; Pfefferlé et al., 1991; Souvignier & Gerwert, 1992; Sasaki et al., 1992), which may be related to those detected by diffraction, appear to lower the pK_a of D96 at this time (Cao et al., 1993), which becomes then a proton donor to the Schiff base. Reprotonation of the now anionic D96 from the cytoplasmic surface may be the step linked to reestablishement of the original *E* conformation (Váró & Lanyi, 1995). Reisomerization of the retinal, and an internal proton transfer that deprotonates D85, complete the recovery of the initial state and the net translocation of a proton.

In *N. pharaonis* halorhodopsin the equivalents of all of these steps are detected, with modifications to accomplish the translocation of a chloride ion instead of a proton, and in the opposite direction. If the *E* ⇔ *C* conformational shift determines the direction of the transport, how does it occur in halorhodopsin? Importantly, in the halorhodopsins the residue at the position of D85 in bacteriorhodopsin is not an aspartate but a threonine, *i.e.*, it is uncharged. This will prevent the loss of the Schiff base proton as the L state is reached, and the trigger for the conformational change in bacteriorhodopsin will be therefore absent. However, the residue analogous to D96 in bacteriorhodopsin is also replaced in the halorhodopsins, by an alanine. The structure of D85N/D96N bacteriorhodopsin, which lacks these two aspartates, was found to be shifted to the *C* conformation even in the unphotolyzed state (Kataoka et al., 1994). Does this kind of conformation describe then the structure of unphotolyzed halorhodopsin? According to the structure of *H. salinarium* halorhodopsin at 7 Å resolution (Havelka et al., 1995), there are some differences in the tilts of helices B, C, F, and G of halorhodopsin relative to those in bacteriorhodopsin, although they are small enough to be at the limit of the resolution (±5°). The main structural difference between the two proteins is in the dispositions of the cytoplasmic ends of helices F and G. This is where the E ⇔ C conformational shift in bacteriorhodopsin occurs. Although the differences are not yet well defined, they do seem to consist of greater distance between helices F and G, and a generally more exposed intrahelical cavity in halorhodopsin than in bacteriorhodopsin. Thus, the structure of unphotolyzed halorhodopsin bears some resemblance to the *C* conformation of bacteriorhodopsin.

It seems possible therefore, that the transient volume *decrease* seen in the halorhodopsin photocycle (Figure 11), which has a magnitude about twice the volume increase in the bacteriorhodopsin photocycle (Váró & Lanyi, 1995), might be the functional equivalent of the *C* → *E* conforma-

tion shift. Since it is detected in the L → N reaction, the analogy with the other protein suggests that at this step the cytoplasmic surface becomes more closed and less accessible to water. We speculate that this transition could cause destabilization of buried positive charges near the cytoplasmic surface, possibly those of R63 and K215 (numbering for *N. pharaonis* halorhodopsin, in Lanyi et al., 1990). In response to this, and the reisomerization of the retinal to all-*trans* in the N → O reaction which follows (Váró et al. 1995b), a chloride ion bound initially near the Schiff base (Schobert & Lanyi, 1986; Pande et al., 1989; Braiman et al., 1994; Walter & Braiman, 1994) would move to the cytoplasmic side and be released there. The origin of the large activation volume at the N ⇔ O equilibrium, unique in the photocycle (Figure 11), could be the need to hydrate the chloride transfer pathway, as observed in the case of proton transfer in the M ⇔ N equilibrium reaction in bacteriorhodopsin (Cao et al., 1991). The M ⇔ N equilibrium reaction in bacteriorhodopsin also has the largest activation volume in the photocycle (Váró & Lanyi, 1995). The red-shift of the maximum in the O state reflects the ensuing decrease in the negative charge of the counter-ion to the Schiff base, as in bacteriorhodopsin. Uptake of a chloride ion in the O → HR′ reaction would restore the initial absorption maximum if this uptake were at the extracellular surface. Evidence was given recently for the role of an arginine residue in this region (R108 in the *H. salinarium* halorhodopsin sequence) in chloride binding (Rüdiger et al., 1995). Although not distinguished by a significant volume change, the enthalpy−entropy conversion at this step (Figure 8) indicates that chemical affinities, perhaps including electrostatic interaction of the chloride with the Schiff base, are satisfied but occur at the expense of a transition to a hindered protein conformation. Recovery of the initial volume, and therefore protein conformation, occurs in either the O → HR′ or the HR′ → HR reaction. Little loss of free energy occurs at any of the reactions between K and HR′. It is therefore the strongly exergonic step in the HR′ → HR step that drives all the thermal reactions in the cycle.

This is a tentative mechanism, meant to be tested in the future by examining the altered photocycles of recombinant proteins where residues that participate in binding the chloride are replaced, as in bacteriorhodopsin. However, even at this stage, the concept that emerges is clear. The transport mechanism is remarkably like that in bacteriorhodopsin, except that many of the steps are the reverse, or occur in the reverse sequence. Chloride release at the cytoplasmic surface followed by uptake at the extracellular surface are analogous to proton release at the extracellular surface in bacteriorhodopsin, followed by uptake at the cytoplasmic side. The apparent open-to-closed conformation change, which we suggest results in the internal chloride transfer from near the Schiff base to the cytoplasmic side, is the reverse of the *E* → *C* conformation change in bacteriorhodopsin that results in internal proton transfer in the reverse direction, from D96 on the cytoplasmic side to the Schiff base. These analogies suggest that the basic features of the ion translocation mechanisms in the two proteins are closely related, if not identical to each other, consistent with the recent finding that replacement of D85 in bacteriorhodopsin with a threonine converted this proton pump into a chloride ion pump (Sasaki et al., 1995).

REFERENCES

Albery, W. J., & Knowles, J. R. (1976) *Biochemistry 15*, 5631−5640.

Alexiev, U., Marti, T., Heyn, M. P., Khorana, H. G., & Scherrer, P. (1994) *Biochemistry 33*, 298−306.

Bivin, D. B., & Stoeckenius, W. (1986) *J. Gen. Microbol. 132*, 2167−2177.

Braiman, M. S., Bousché, O., & Rothschild, K. J. (1991) *Proc. Natl. Acad. Sci. U.S.A. 88*, 2388−2392.

Braiman, M. S., Walter, T. J., & Briercheck, D. M. (1994) *Biochemistry 33*, 1629−1635.

Cao, Y., Váró, G., Chang, M., Ni, B., Needleman, R., & Lanyi, J. K. (1991) *Biochemistry 30*, 10972−10979.

Cao, Y., Váró, G., Klinger, A. L., Czajkowsky, D. M., Braiman, M. S., Needleman, R., & Lanyi, J. K. (1993) *Biochemistry 32*, 1981−1990.

Cao, Y., Brown, L. S., Sasaki, J., Maeda, A., Needleman, R., & Lanyi, J. K. (1995) *Biophys. J. 68*, 1518−1530.

Dencher, N. A., Dresselhaus, D., Zaccai, G., & Büldt, G. (1989) *Proc. Natl. Acad. Sci. U.S.A. 86*, 7876−7879.

Duschl, A., Lanyi, J. K., & Zimányi, L. (1990) *J. Biol. Chem. 265*, 1261−1267.

Fodor, S. P., Bogomolni, R. A., & Mathies, R. A. (1987) *Biochemistry 26*, 6775−6778.

Gross, M., & Jaenicke, R. (1994) *Eur. J. Biochem. 221*, 617−630.

Han, B.-G., Vonck, J., & Glaeser, R. M. (1994) *Biophys. J. 67*, 1179−1186.

Havelka, W. A., Henderson, R., & Oesterhelt, D. (1995) *J. Mol. Biol. 247*, 726−738.

Heberle, J., & Dencher, N. A. (1992) *Proc. Natl. Acad. Sci. U.S.A. 89*, 5996−6000.

Heremans, K. (1982) *Annu. Rev. Biophys. Bioeng. 11*, 1−21.

Kataoka, M., Kamikubo, H., Tokunaga, F., Brown, L. S., Yamazaki, Y., Maeda, A., Sheves, M., Needleman, R., & Lanyi, J. K. (1994) *J. Mol. Biol. 243*, 621−638.

Koch, M. H. J., Dencher, N. A., Oesterhelt, D., Plöhn, H.-J., Rapp, G., & Büldt, G. (1991) *EMBO J. 10*, 521−526.

Lanyi, J. K. (1986) *Annu. Rev. Biophys. Biophys. Chem. 15*, 11−28.

Lanyi, J. K. (1990) *Physiol. Rev. 70*, 319−330.

Lanyi, J. K., Duschl, A., Hatfield, G. W., May, K. M., & Oesterhelt, D. (1990) *J. Biol. Chem. 265*, 1253−1260.

Liu, S. Y. (1990) *Biophys. J. 57*, 943−950.

Liu, S. Y., Govindjee, R., & Ebrey, T. G. (1990) *Biophys. J. 57*, 951−963.

Marque, J., & Eisenstein, L. (1984) *Biochemistry. 23*, 5556−5563.

Marti, T., Otto, H., Rösselet, S. J., Heyn, M. P., & Khorana, H. G. (1992) *J. Biol. Chem. 267*, 16922−16927.

Miller, A., & Oesterhelt, D. (1990) *Biochim. Biophys. Acta 1020*, 57−64.

Nakasako, M., Kataoka, M., Amemiya, Y., & Tokunaga, F. (1991) *FEBS Lett. 292*, 73−75.

Oesterhelt, D., & Tittor, J. (1989) *TIBS 14*, 57−61.

Oesterhelt, D., Tittor, J., & Bamberg, E. (1992) *J. Bioenerg. Biomembr. 24*, 181−191.

Otomo, J., Tomioka, H., & Sasabe, H. (1992) *Biochim. Biophys. Acta 1112*, 7−13.

Otto, H., Marti, T., Holz, M., Mogi, T., Lindau, M., Khorana, H. G., & Heyn, M. P. (1989) *Proc. Natl. Acad. Sci. U.S.A. 86*, 9228−9232.

Pande, C., Lanyi, J. K., & Callender, R. H. (1989) *Biophys. J. 55*, 425−431.

Pfefferlé, J.-M., Maeda, A., Sasaki, J., & Yoshizawa, T. (1991) *Biochemistry 30*, 6548−6556.

Rothschild, K. J., Zagaeski, M., & Cantore, W. A. (1981) *Biochem. Biophys. Res. Commun. 103*, 483−489.

Rothschild, K. J., Bousche, O., Braiman, M. S., Hasselbacher, C. A., & Spudich, J. L. (1988) *Biochemistry 27*, 2420−2424.

Rüdiger, M., Haupts, U., Gerwert, K., & Oesterhelt, D. (1995) *EMBO J. 14*, 1599−1606.

Sasaki, J., Shichida, Y., Lanyi, J. K., & Maeda, A. (1992) *J. Biol. Chem. 267*, 20782−20786.

Sasaki, J., Brown, L. S., Chon, Y.-S., Kandori, H., Maeda, A., Needleman, R., & Lanyi, J. K. (1995) *Science 269*, 73−75.

Scharf, B., & Engelhard, M. (1994) *Biochemistry 33*, 6387−6393.

Schobert, B., & Lanyi, J. K. (1982) *J. Biol. Chem. 257*, 10306−10313.
Schobert, B., & Lanyi, J. K. (1986) *Biochemistry 25*, 4163−4167.
Soppa, J., Duschl, J., & Oesterhelt, D. (1993) *J. Bacteriol. 175*, 2720−2726.
Souvignier, G., & Gerwent, K. (1992) *Biophys. J. 63*, 1393−1405.
Subramaniam, S., Gerstein, M., Oesterhelt, D., & Henderson, R. (1993) *EMBO J. 12*, 1−8.
Tittor, J., Soell, C., Oesterhelt, D., Butt, H.-J., & Bamberg, E. (1989) *EMBO J. 8*, 3477−3482.
Váró, G., & Lanyi, J. K. (1991a) *Biochemistry 30*, 5016−5022.
Váró, G., & Lanyi, J. K. (1991b) *Biochemistry 30*, 7165−7171.
Váró, G., & Lanyi, J. K. (1995) *Biochemistry* (in press).
Váró, G., Zimányi, L., Fan, X., Sun, L., Needleman, R., & Lanyi, J. K. (1995a) *Biophys. J. 68*, 2062−2072.
Váró, G., Brown, L. S., Sasaki, J., Kandori, H., Maeda, A., Needleman, R., & Lanyi, J. K. (1995b) *Biochemistry 34*, 14490−14499.
Walter, T. J., & Braiman, M. S. (1994) *Biochemistry 33*, 1724−1733.
Zimányi, L., & Lanyi, J. K. (1993) *Biophys. J. 64*, 240−251.
Zimányi, L., Keszthelyi, L., & Lanyi, J. K. (1989) *Biochemistry 28*, 5165−5172.
Zimányi, L., Váró, G., Chang, M., Ni, B., Needleman, R., & Lanyi, J. K. (1992) *Biochemistry 31*, 8535−8543.
Zimányi, L., Cao, Y., Needleman, R., Ottolenghi, M., & Lanyi, J. K. (1993) *Biochemistry 32*, 7669−7678.

BI9514673